

Chemo- and Periselectivity in the Addition of $[\text{OsO}_2(\text{CH}_2)_2]$ to Ethylene: A Theoretical Study

Markus Hölscher,^[a] Walter Leitner,^[a] Max C. Holthausen,*^[b] and Gernot Frenking*^[b]

Abstract: Quantum chemical calculations by using density functional theory at the B3LYP level have been carried out to elucidate the reaction course for the addition of ethylene to $[\text{OsO}_2(\text{CH}_2)_2]$ (**1**). The calculations predict that the kinetically most favorable reaction proceeds with an activation barrier of $8.1 \text{ kcal mol}^{-1}$ via [3+2] addition across the $\text{O}=\text{Os}=\text{CH}_2$ moiety. This reaction is $-42.4 \text{ kcal mol}^{-1}$ exothermic. Alternatively, the [3+2] addition to the $\text{H}_2\text{C}=\text{Os}=\text{CH}_2$ fragment of **1** leads to the most stable addition product **4** ($-72.7 \text{ kcal mol}^{-1}$), yet this process has a higher activation barrier (13.0 kcal

mol^{-1}). The [3+2] addition to the $\text{O}=\text{Os}=\text{O}$ fragment yielding **2** is kinetically ($27.5 \text{ kcal mol}^{-1}$) and thermodynamically ($-7.0 \text{ kcal mol}^{-1}$) the least favorable [3+2] reaction. The formal [2+2] addition to the $\text{Os}=\text{O}$ and $\text{Os}=\text{CH}_2$ double bonds proceeds by initial rearrangement of **1** to the metallaoxirane **1a**. The rearrangement **1**→**1a** and the following [2+2] additions have significantly higher activation barriers

($>30 \text{ kcal mol}^{-1}$) than the [3+2] reactions. Another isomer of **1** is the dioxosmacyclopropane **1b**, which is $56.2 \text{ kcal mol}^{-1}$ lower in energy than **1**. The activation barrier for the **1**→**1b** isomerization is $15.7 \text{ kcal mol}^{-1}$. The calculations predict that there are no energetically favorable addition reactions of ethylene with **1b**. The isomeric form **1c** containing a peroxy group is too high in energy to be relevant for the reaction course. The accuracy of the B3LYP results is corroborated by high level post-HF CCSD(T) calculations for a subset of species.

Keywords: density functional calculations • carbenes • osmium • oxidation • reaction mechanisms

Introduction

The addition of OsO_4 to olefins yielding *cis*-diols is an important reaction in synthetic organometallic chemistry.^[1] Its synthetic utility became much broader through the pioneering studies of Sharpless^[2] who developed protocols for the enantioselective synthesis of diols in the presence of chiral bases using catalytic amounts of OsO_4 . The mechanism of the reaction has been revealed by high-level quantum chemical calculations.^[3] The scope of the reaction became even larger when monoimido derivatives $[\text{OsO}_3(\text{NR})]$ were suc-

cessfully used for the enantioselective addition to prochiral olefins yielding vicinal aminoalcohols after hydrolysis.^[4] It appears that other variants of the reaction are still awaiting exploration. Deubel and Muñiz recently reported theoretical studies of the reaction pathways of the addition of $[\text{OsO}_2(\text{NH})_2]$ to ethylene.^[5] The calculations predict that the three possible [3+2] addition reactions are kinetically and thermodynamically favored over the two [2+2] additions, and that the diamination should be the most favored reaction. Pioneering experimental studies of the diamination of olefins with osmium trisimido compounds $[\text{OsO}(\text{NR})_3]$ have recently been reported by Muñiz.^[6] An important contribution to the ongoing research^[7] about competitive [3+2] and [2+2] addition of olefins to transition metal oxo compounds has recently been made by Chen et al. who reported experimental and theoretical results of a reaction where a [2+2] addition is favored over a [3+2] addition.^[8]

In this paper we present the first quantum chemical investigation of the addition of the bisalkylidene $[\text{OsO}_2(\text{CH}_2)_2]$ to ethylene. We explored a variety of conceivable pathways for this system in view of its potential synthetic relevance. For example, if the reaction would proceed via [3+2] addition of C_2H_4 to the $\text{H}_2\text{C}=\text{Os}=\text{CH}_2$ moiety, two C–C bonds would be

[a] Dr. M. Hölscher, Prof. W. Leitner
Institut für Technische und Makromolekulare Chemie
Rheinisch-Westfälische Technische Hochschule Aachen
Worringer Weg 1, 52074 Aachen (Germany)

[b] Dr. M. C. Holthausen, Prof. G. Frenking
Fachbereich Chemie, Philipps-Universität Marburg
Hans-Meerwein-Strasse, 35043 Marburg (Germany)
Fax: (+49) 6421-282-5566
E-mail: Max.Holthausen@chemie.uni-marburg.de
Frenking@chemie.uni-marburg.de

Supporting information for this article is available on the WWW under <http://www.chemeurj.org/> or from the author.

formed just as in a Diels–Alder reaction. Such a reaction could be very useful because the choice of substituted olefins and other carbenes would allow access to a wide variety of organic compounds.

Computational Methods

Calculations at the density functional theory (DFT) level have been performed employing the B3LYP hybrid functional^[9] as implemented^[10] in the Gaussian 03 program.^[11] The TZVP all electron basis set of Ahlrichs and co-workers was employed for C, O, and H.^[12] For Os the Stuttgart/Köln relativistic effective core potential replacing 60 core electrons was used in combination with a (311111/22111/411) valence basis.^[13] This combination is denoted as basis set I. All minima and transition structures were optimized at this level of theory without symmetry constraints. Analytic Hessians computed at B3LYP/I were used to characterize the nature of stationary points and to obtain (unscaled) zero-point vibrational energy contributions (ZPE). All connectivities of minima and transition structures implied in the figures below were verified by intrinsic reaction coordinate (IRC) following calculations at this level of theory. Based on the B3LYP/I geometries additional single point calculations were employed by using a larger basis set where the Stuttgart/Köln valence basis for Os was augmented by two sets of *f* functions and one set of *g* functions derived by Martin and Sundermann.^[14] This was combined with the correlation consistent cc-pVTZ basis set of Dunning^[15] for C, O, and H atoms and this one particle basis is referred to as basis set II. We also carried out calculations at the CCSD(T)/II level of theory^[16] using B3LYP/I optimized geometries for a subset of species to establish the accuracy of the B3LYP data. In the CCSD(T) calculations the 1s core electrons of C and O as well as the 5s and 5p electrons of Os were not included in the correlation treatment. CCSD(T) calculations were performed using the Molpro program.^[17] Unless specified otherwise energies discussed in this paper relate to B3LYP/II calculations. Relative energies include ZPE contributions.

Results and Discussion

All optimized equilibrium structures and transition states and the most important bond lengths are shown in Figure 1. Cartesian coordinates of all stationary points are provided as Supporting Information. Table 1 contains the absolute and relative energies of the calculated structures. The theoretically predicted reaction courses for the [3+2] and [2+2] addition are displayed in Figure 2.

We investigated three different pathways for the [3+2] addition of C₂H₄ to [OsO₂(CH₂)₂] (**1**), corresponding to three different chemoselectivities. The products dimethyleneosma-2,5-dioxolane (**2**), methyleneoxosma-2-oxolane (**3**), and dioxosmacyclopentane (**4**) are formed by addition of ethylene across the O=Os=O, O=Os=CH₂, and H₂C=Os=CH₂ moieties, respectively. First of all we note an unexpected trend in the theoretically predicted activation barriers. The calculated activation energy for the [3+2] addition across the O=Os=O moiety of **1** is rather high (27.5 kcal mol⁻¹, **TS1**→**2**), much higher than the previously calculated barriers for the [3+2] addition across the O=Os=O moieties of OsO₄ (11.8 kcal mol⁻¹)^[18] and [OsO₂(NH)₂] (8.3 kcal mol⁻¹).^[5] The theoretically predicted energy barriers for the [3+2] additions to the O=Os=CH₂ (8.1 kcal mol⁻¹, **TS1**→**3**)

and H₂C=Os=CH₂ (13.0 kcal mol⁻¹, **TS1**→**4**) fragments are much smaller. Hence we find that the activation barriers for the [3+2] additions decrease in the order O=Os=O > H₂C=Os=CH₂ > O=Os=CH₂ (Figure 2). This is different from the analogous [3+2] addition of ethylene to [OsO₂(NH)₂] for which the trend O=Os=O > O=Os=NH > HN=Os=NH has been reported.^[5] In this context we note that the [3+2] addition **1**→**4** has a higher activation barrier than the reaction **1**→**3** although the former process is much more endothermic (−72.7 kcal mol⁻¹) than the latter (−42.4 kcal mol⁻¹). Thus, under kinetic control the [3+2] addition should yield **3** as the reaction product while under thermodynamic control it should lead to **4**. Addition of ethylene across the O=Os=O moiety along the path **1**→**2** is the least favored [3+2] addition reaction, both kinetically and thermodynamically (Table 1).

In the course of searching for transition states of the [3+2] addition pathways we additionally found two transition states belonging to totally different reaction routes. In transition state **TS1**→**5** shown in Figure 1 one of the oxo ligands of **1** becomes bonded to the attacking ethylene while a hydrogen atom of one carbene migrates to ethylene to yield the alkoxy–alkylidene complex **5**. The resulting reaction **1**→**5** is −12.6 kcal mol⁻¹ exothermic with a moderate activation barrier of 21.2 kcal mol⁻¹ (Table 1). We identified a related transition state for the formation of an analogous alkylidene–alkylidene complex **6** as a higher order saddle point (three imaginary frequencies) without chemical relevance. Thus, unlike the reaction **1**→**5**, formation of **6** does not take place by a concerted addition/hydrogen migration reaction of ethylene and **1**. Instead, we identified **TS4**→**6** (Figure 1) as a transition state for the formation of **6** and IRC calculations endorse its direct connection to **4**. However, starting from **4**, this process corresponds to a highly endothermic rearrangement and is thus unlikely to take place.

We also searched for the transition states of the [2+2] additions of ethylene to **1** across the Os=O and Os=CH₂ bonds to yield the methyleneoxosma-2-oxetane (**7**) or methylenedioxosmacyclobutane (**8**), respectively. Closer inspection of the transition modes in the related transition states as well as careful IRC calculations showed that, preceding the formation of **7** and **8**, compound **1** rearranges to the isomer **1a** which is 17.6 kcal mol⁻¹ lower in energy than **1** (Table 1). Isomer **1a** is formed via coupling of one oxygen atom with one methylene group yielding an osmaoxirane. Related metallaoxiranes are well known^[19] and have been postulated to occur under special conditions^[20] as intermediates in the McMurry reaction.^[21] Yet, for the present system we find that the activation barrier for the rearrangement **1**→**1a** is rather high (40.9 kcal mol⁻¹). In addition, the subsequent activation barriers for the formal [2+2] addition reactions **1a**→**7** (41.3 kcal mol⁻¹) and **1a**→**8** (34.8 kcal mol⁻¹) are substantial. As both reactions are also endothermic with respect to **1a**, we conclude that they are unlikely to occur for kinetic as well as thermodynamic reasons. Alternatively, **7** is also accessible through rearrangement of **3**. But the transition state **TS7**→**3** is also high in energy (58.9 kcal mol⁻¹ with re-

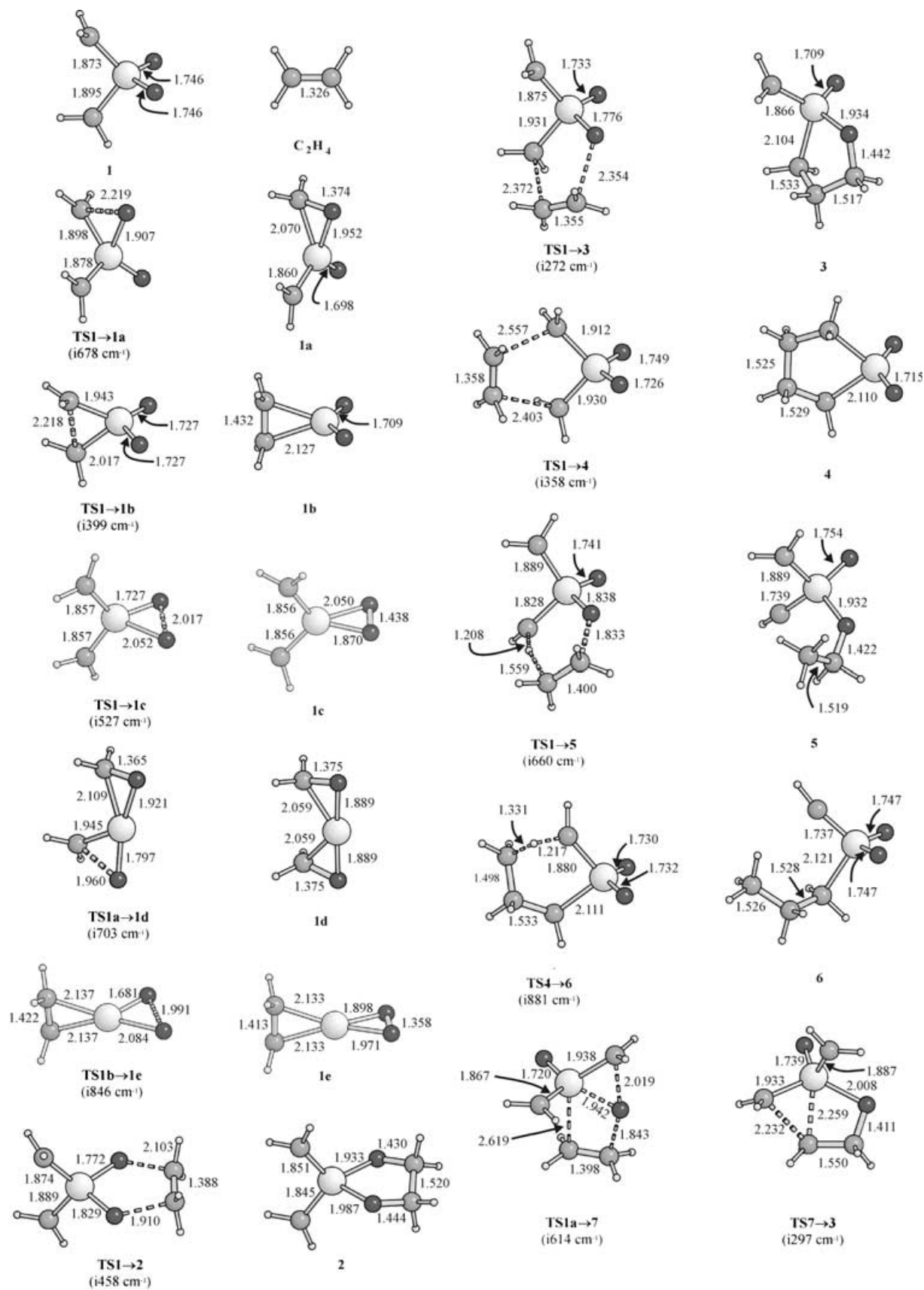


Figure 1. Optimized equilibrium and transition state structures. Calculated bond lengths [Å], and imaginary transition modes at B3LYP/I.

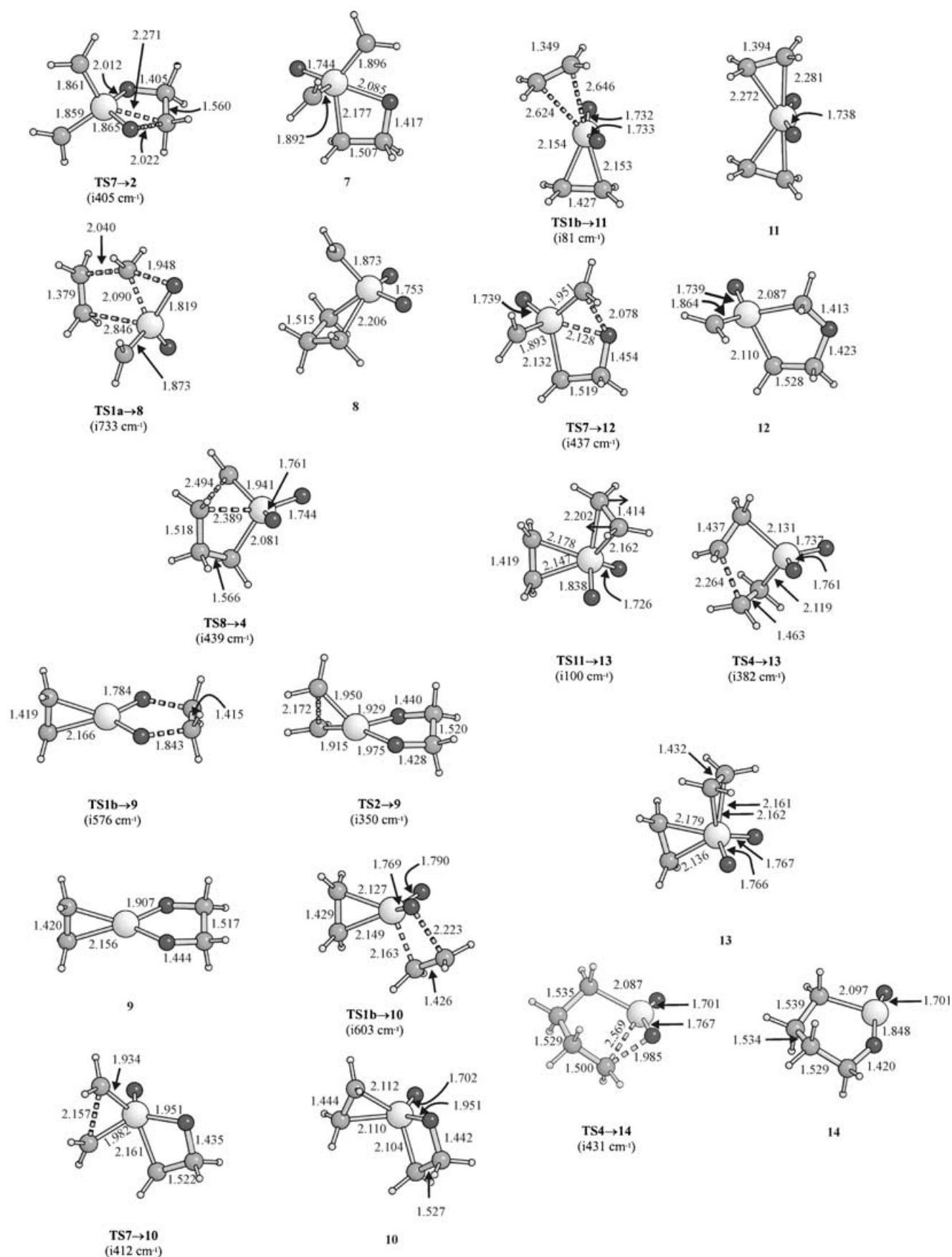


Figure 1 (continued).

spect to **3**), which indicates that this reaction probably also does not take place.

The calculated reaction profiles for the [3+2] addition reactions **1**→**2**, **1**→**3** and **1**→**4**, the addition reaction with concomitant hydrogen migration **1**→**5** as well as the formal [2+2] additions **1**→**1a**→**7** and **1**→**1a**→**8** are shown in Figure 2, which displays the most important theoretical findings discussed so far. From this comparison it becomes obvious that the [3+2] addition across the O=Os=CH₂ **1**→**3** moiety is kinetically favored over all other reaction pathways while the [3+2] addition **1**→**4** is the thermodynamically most favored reaction. The activation barrier for the [3+2] addition **1**→**4** (13.0 kcal mol⁻¹) is also rather low, whereas the addition/hydrogen migration process **1**→**5**

(21.2 kcal mol⁻¹) and the reaction **1**→**2** (27.5 kcal mol⁻¹) have higher activation barriers. The remaining reactions shown have even larger activation barriers.

The serendipitous finding of isomer **1a** with a C–O bond led us to search for other isomers of **1**, which might open further reaction pathways that are energetically feasible. Indeed, we identified an energetically low lying osmacyclopropane isomer (**1b**, Figure 1), in which a C–C bond between the former carbene ligands is present. Remarkably, **1b** is more stable than **1** by 56.2 kcal mol⁻¹ (Table 1) and represents the lowest energy isomer on the OsO₂C₂H₄ PES (cf. Figure 1). The activation barrier for the rearrangement **1**→**1b** via **TS1**→**1b** amounts to only 15.7 kcal mol⁻¹. Interestingly, however, this barrier is higher than the activation

barrier for the [3+2] addition of **1** with ethylene yielding **3** (8.1 kcal mol⁻¹). We also identified a peroxo isomer **1c**, which is 64.6 kcal mol⁻¹ less stable than **1**. The O–O bond formation via **TS1**→**1c** is connected with a huge activation barrier of 88.5 kcal mol⁻¹. Starting from **1b** a related rearrangement to form the bicyclic isomer **1e** (which is 60.3 kcal mol⁻¹ less stable than **1**) is connected with an even larger barrier, that is, 150.2 kcal mol⁻¹ with respect to **1b**. Finally, isomerization of **1a** yields **1d**, which is 0.7 kcal mol⁻¹ lower in energy than **1** but 55.5 kcal mol⁻¹ less stable than **1b** or 15.0 kcal mol⁻¹ less stable than **1a**, respectively. The transition state **TS1a**→**1d** connecting **1a** with **1d** is rather high in energy (34.2 kcal mol⁻¹, Table 1).

Next, we investigated possible [3+2] and [2+2] addition reactions of ethylene to the osmacyclopropane species **1b**. The calculated reaction profiles for the three reactions starting from **1b** are shown in Figure 3. The [3+2] addition across the O=Os=O moiety of **1b** leading to the bicyclic product **9** is a highly endothermic reaction which possesses a large activation barrier with respect to **1b** (Table 1, Figure 3). The [2+2] addition to the Os=O bond of **1b** to yield another bicyclic molecule **10** is thermodynamically nearly neutral but the

Table 1. Calculated energies. Total energies are given in Hartrees, relative energies in kcal mol⁻¹; E_{rel}^0 include zero point vibrational energy contributions obtained at the B3LYP/I level.

Structure	B3LYP/I			B3LYP/II//B3LYP/I		
	E_{tot}	E_{rel}	E_{rel}^0	E_{tot}	E_{rel}	E_{rel}^0
C ₂ H ₄	-78.62155	-	-	-78.62317	-	-
1	-319.77744	0.0 ^[a]	0.0 ^[a]	-319.81727	0.0 ^[a]	0.0 ^[a]
TS1 → 1a	-319.71744	37.7 ^[a]	37.0 ^[a]	-319.75093	41.6 ^[a]	40.9 ^[a]
1a	-319.81307	-22.4 ^[a]	-20.9 ^[a]	-319.84753	-19.0 ^[a]	-17.6 ^[a]
TS1 → 1b	-319.75383	14.8 ^[a]	14.9 ^[a]	-319.79246	15.6 ^[a]	15.7 ^[a]
1b	-319.87437	-60.8 ^[a]	-57.7 ^[a]	-319.91186	-59.4 ^[a]	-56.2 ^[a]
TS1 → 1c	-319.64011	86.2 ^[a]	84.0 ^[a]	-319.67284	90.6 ^[a]	88.5 ^[a]
1c	-319.68217	59.8 ^[a]	58.2 ^[a]	-319.71173	66.2 ^[a]	64.6 ^[a]
TS1a → 1d	-319.73431	27.1 ^[a]	28.8 ^[a]	-319.76544	32.5 ^[a]	34.2 ^[a]
1d	-319.79544	-11.3 ^[a]	-7.7 ^[a]	-319.82418	-4.3 ^[a]	-0.7 ^[a]
TS1b → 1e	-319.64352	84.0 ^[a]	85.3 ^[a]	-319.66939	92.8 ^[a]	94.0 ^[a]
1e	-319.70381	46.2 ^[a]	48.4 ^[a]	-319.72454	58.0 ^[a]	60.3 ^[a]
TS1 → 2	-398.36416	21.9	22.8	-398.39825	26.5	27.5
2	-398.42714	-17.7	-14.6	-398.45652	-10.1	-7.0
TS1 → 3	-398.39207	4.3	6.1	-398.43019	6.4	8.1
3	-398.48446	-53.6	-47.9	-398.51712	-48.1	-42.4
TS1 → 4	-398.38063	11.5	12.4	-398.42106	12.2	13.0
4	-398.53078	-82.7	-75.4	-398.56788	-80.0	-72.7
TS1 → 5	-398.36920	18.7	18.7	-398.40671	21.2	21.2
5	-398.42959	-19.2	-15.8	-398.46599	-16.0	-12.6
TS4 → 6	-398.41760	-11.7	-8.9	-398.45640	-10.0	-7.2
6	-398.44977	-31.9	-27.6	-398.49088	-31.7	-27.3
TS1a → 7	-398.34010	36.9	38.1	-398.37657	40.1	41.3
TS7 → 2	-398.35201	29.5	31.4	-398.38421	35.3	37.3
TS7 → 3	-398.38536	8.5	12.1	-398.41984	12.9	16.5
7	-398.39992	-0.6	2.9	-398.43302	4.7	8.1
TS1a → 8	-398.34999	30.7	32.6	-398.38784	33.0	34.8
8	-398.42183	-14.3	-10.0	-398.46154	-13.2	-8.9
TS8 → 4	-398.38421	9.3	13.2	-398.42310	10.9	14.8
TS1b → 9	-398.40692	-5.0	-0.6	-398.43356	4.3	8.7
TS2 → 9	-398.39739	1.0	5.6	-398.42218	11.5	16.0
9	-398.43705	-23.9	-17.4	-398.45845	-11.3	-4.8
TS1b → 10	-398.41527	-10.2	-6.5	-398.44810	-4.8	-1.1
TS7 → 10	-398.38302	10.0	13.8	-398.41960	13.1	16.8
10	-398.49782	-62.0	-55.9	-398.53176	-57.3	-51.2
TS1b → 11	-398.48978	-57.0	-52.3	-398.52889	-55.5	-50.8
11	-398.49079	-57.6	-52.5	-398.52994	-56.2	-51.1
TS7 → 12	-398.37527	14.9	18.3	-398.40754	20.6	24.0
12	-398.46492	-41.4	-36.3	-398.49373	-33.4	-28.3
TS4 → 13	-398.41639	-10.9	-6.0	-398.45383	-8.4	-3.4
TS11 → 13	-398.44784	-30.7	-25.7	-398.48326	-26.9	-21.9
13	-398.45551	-35.5	-30.3	-398.49227	-32.5	-27.3
TS4 → 14	-398.45762	-36.8	-30.5	-398.49375	-33.5	-27.2
14	-398.49381	-59.5	-51.4	-398.52679	-54.2	-46.1

[a] Relative energies including C₂H₄.

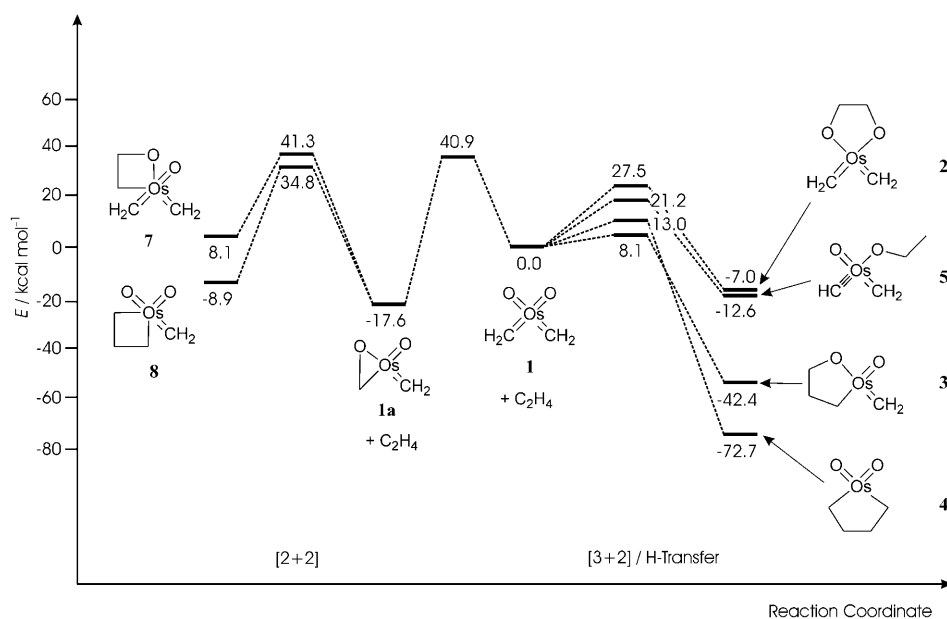


Figure 2. Theoretically predicted reaction profile at B3LYP/II//B3LYP/I for the [3+2] cycloaddition and hydrogen migration/C–C addition (right-hand side) of C_2H_4 to $[OsO_2(CH_2)_2]$ (**1**). The left-hand side shows the [2+2] additions of ethylene via the isomer **1a**. Energy values are given in $kcal\ mol^{-1}$.

transition state **TS1b**→**10** is connected with a high activation barrier of $55.1\ kcal\ mol^{-1}$. We identified a loosely bound ethylene complex **11**, in which the ligand is directly bonded to the metal (Figure 1). However, as the activation barrier for the loss of ethylene amounts to merely $0.3\ kcal\ mol^{-1}$, **11** represents only a kinetically stable species. Overall it is evident that the energetically lowest isomer **1b** is a dead end for further addition reactions.

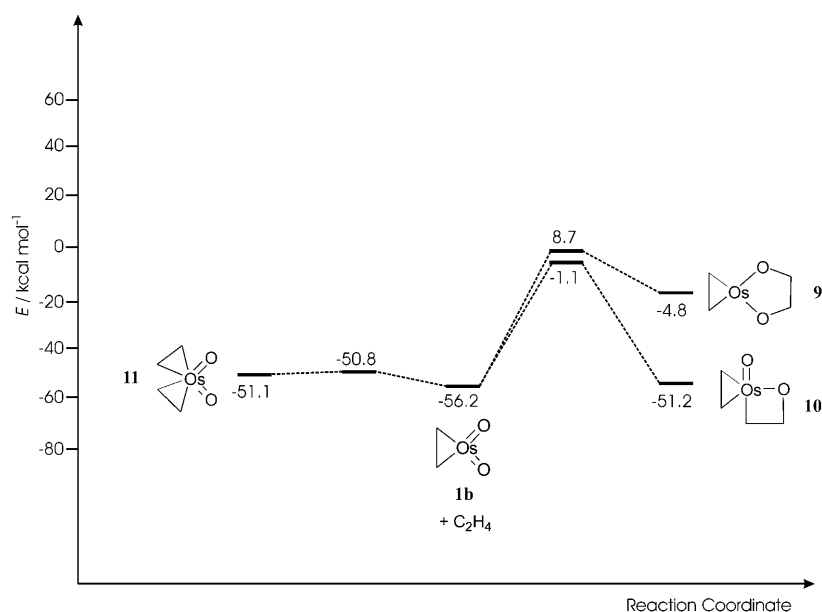


Figure 3. Theoretically predicted reaction profile at B3LYP/II//B3LYP/I for the addition of C_2H_4 to **1b**. Energy values are given in $kcal\ mol^{-1}$.

Finally, we searched for other reactions between C_2H_4 and either **1** or its isomers as well as for pathways interconnecting the reaction products. Figure 4 summarizes the results and provides an overview of all intermediates and transition state structures identified in the present study. Indeed, via **TS7**→**2**, **TS7**→**3**, or **TS8**→**4** we found several routes along which **7** and **8**, the products of the formal [2+2] addition reactions, may rearrange to the [3+2] products **2**–**5**. But these pathways all have much higher barriers than the direct [3+2] addition reactions. Compound **7** may also rearrange with a moderate activation barrier of $15.9\ kcal\ mol^{-1}$ via **TS7**→**12** to the more stable five-membered cyclic complex **12**, which is $36.4\ kcal\ mol^{-1}$ lower in energy.

The global energy minimum structure **4** may interconvert via intermediate **13** to **11**, which would yield **1b** after loss of ethylene. In the opposite direction, this route would correspond to a multi-step reaction starting from **1** and ethylene yielding **4**, which has little practical relevance, however, because the direct [3+2] addition $C_2H_4 + \mathbf{1} \rightarrow \mathbf{4}$ has a much lower activation barrier. Another rearrangement reaction of **4** yields the relatively low-lying isomer **14** via **TS4**→**14**.

Overall it is apparent from the B3LYP/II calculations that the kinetically most favorable reaction of **1** with ethylene proceeds via [3+2] addition across the $O=Os=CH_2$ moiety yielding **3** as reaction product. The activation barrier for the reaction is $8.1\ kcal\ mol^{-1}$. The kinetically next higher-lying process with a barrier of $13.0\ kcal\ mol^{-1}$ is the [3+2] addition across the $H_2C=Os=CH_2$ fragment, which leads to the thermodynamically most stable product **4**. The isomerization of **1** to the much more stable species **1b** which has an activation barrier of $15.7\ kcal\ mol^{-1}$ is a dead end because the addition reactions of the latter isomer with ethylene are energetically unfavorable. The calculated alternative routes are kinetically as well as thermodynamically less favorable than

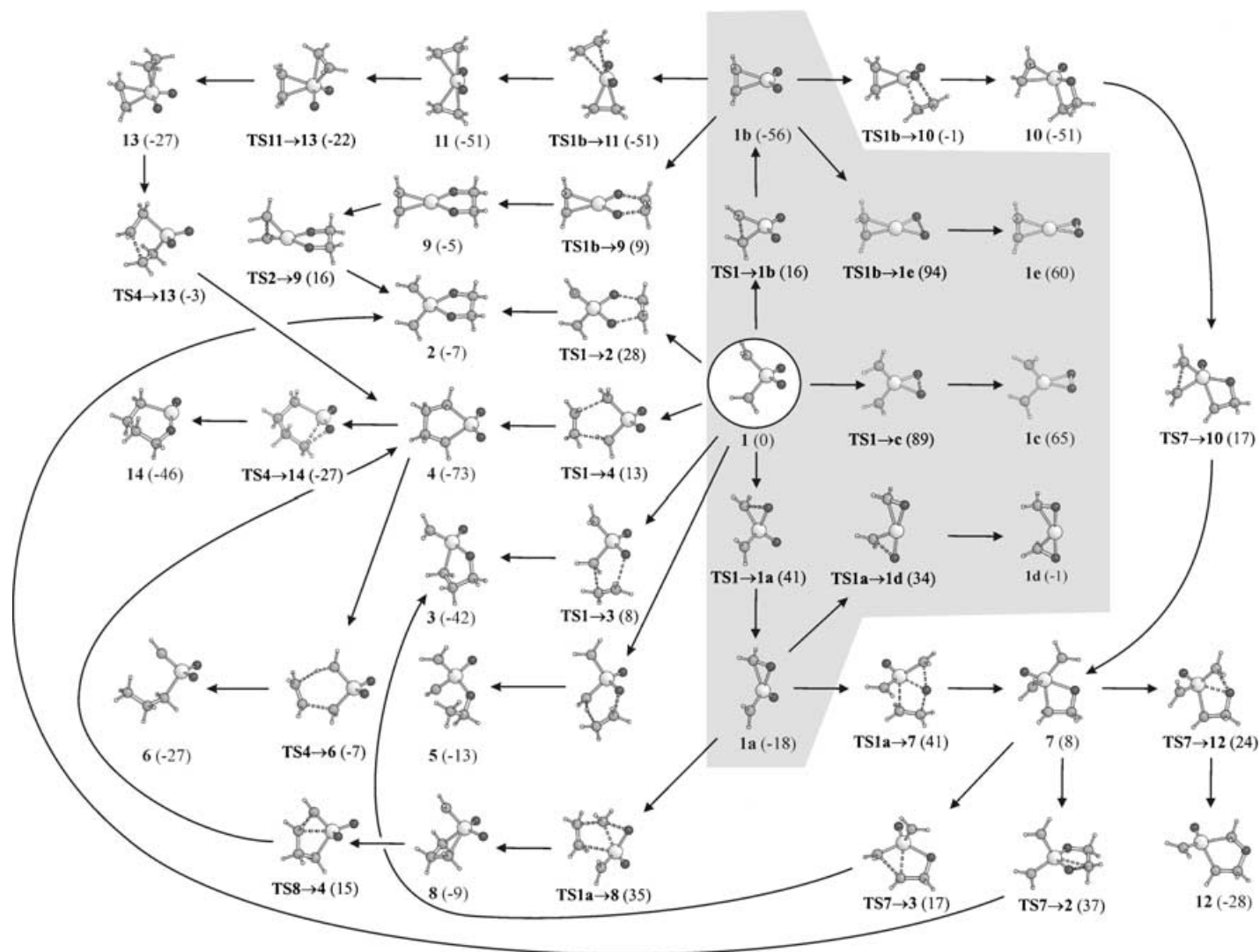


Figure 4. Overview of calculated reaction pathways identified at B3LYP/II//B3LYP/I for the reaction of ethylene with **1**. Energies are given relative to separated **1** + C₂H₄ (including zero point vibrational energy contributions) in kcal mol⁻¹.

these three elementary reactions. It should be noted, however, that the former three reactions may become kinetically competitive at elevated temperatures where entropic and dynamic effects play an important role. Structure **1b** may then react with further oxidation reagents yielding metal-(VIII) compounds which would open new reaction pathways. The latter possibility will be the focus of further theoretical investigations.

In order to estimate the accuracy of the B3LYP values we carried out coupled-cluster calculations at the CCSD(T)/II//B3LYP/I level for selected energy minima and transition states. Table 2 presents the calculated energies without ZPE corrections. It is gratifying that the results at CCSD(T)/II agree nicely with the B3LYP/II values, which substantiates the reliability of the chosen level of DFT for the present system. In particular, the relative energies of the lowest-lying transition states **TS1**→**3**, **TS1**→**4** and **TS1**→**1b** change only slightly when going from B3LYP/II to CCSD(T)/II.

Table 2 also presents *TI* diagnostics^[22] as a means to judge the reliability of the coupled cluster calculations. Although almost all *TI* diagnostics obtained significantly exceed the value of 0.02 recommended by Lee and Taylor for a CCSD calculation to be reliable,^[22] they by and large meet the somewhat relaxed recommendation of *TI* = 0.04 for a CCSD(T) treatment.^[23] The only exception is **TS1b**→**1e**, for which a large *TI* diagnostic of 0.113 clearly indicates the presence of particularly prominent near-degeneracy effects, which render the CCSD(T) results unreliable. Accordingly, the largest deviation between the two levels of theory is found for this species: the activation barrier at CCSD(T)/II (72.1 kcal mol⁻¹) is 20.7 kcal mol⁻¹ lower than that obtained at B3LYP/II (92.8 kcal mol⁻¹). Given its exceedingly high relative energy, however, this transition state is of no relevance for the course of the reaction anyway.

Table 2. Calculated total and relative energies for selected isomers of **1**. Calibration of DFT results against CCSD(T) data.

	B3LYP/I		B3LYP/II//B3LYP/I		CCSD(T)/II//B3LYP/I		<i>T1</i> ^[c]
	<i>E</i> _{tot} ^[a]	<i>E</i> _{rel} ^[b]	<i>E</i> _{tot} ^[a]	<i>E</i> _{rel} ^[b]	<i>E</i> _{tot} ^[a]	<i>E</i> _{rel} ^[b]	
1	-319.77744	0.0	-319.81727	0.0	-318.81723	0.0	0.038
TS1 → 1a	-319.71744	37.7	-319.75093	41.6	-318.74754	43.7	0.046
1a	-319.81307	-22.4	-319.84753	-19.0	-318.84271	-16.0	0.030
TS1 → 1b	-319.75383	14.8	-319.79246	15.6	-318.79343	14.9	0.039
1b	-319.87437	-60.8	-319.91186	-59.4	-318.91068	-58.6	0.030
TS1 → 1c	-319.64011	86.2	-319.67284	90.6	-318.67773	87.5	0.069
1c	-319.68217	59.8	-319.71173	66.2	-318.70468	70.6	0.037
TS1a → 1d	-319.73431	27.1	-319.76544	32.5	-318.76270	34.2	0.046
1d	-319.79544	-11.3	-319.82418	-4.3	-318.81831	-0.7	0.033
TS1b → 1e	-319.64352	84.0	-319.66939	92.8	-318.70138	72.1	0.113
1e	-319.70381	46.2	-319.72454	58.2	-318.72097	60.4	0.068
C ₂ H ₄	-78.62155		-78.62317		-78.43866		0.011
TS1 → 3	-398.39207	4.3	-398.43019	6.4	-397.24996	3.7	0.044
TS1 → 4	-398.38063	11.5	-398.42106	12.2	-397.24063	9.6	0.035

[a] In Hartrees. [b] In kcal mol⁻¹. [c] *T1* diagnostic of Lee and Taylor.^[22]

Summary and Conclusion

The calculated pathways for the addition reaction of ethylene to the bisalkylidene compound [OsO₂(CH₂)₂] show that the kinetically most favorable reaction proceeds with an activation barrier of 8.1 kcal mol⁻¹ via [3+2] addition across the O=Os=CH₂ moiety yielding **3** as the reaction product. This reaction is strongly exothermic by -42.4 kcal mol⁻¹. The [3+2] addition to the H₂C=Os=CH₂ moiety of **1** leads to the most stable addition product **4** (-72.7 kcal mol⁻¹) but this process has a higher activation barrier of 13.0 kcal mol⁻¹. The [3+2] addition to the O=Os=O fragment yielding **2** is kinetically (27.5 kcal mol⁻¹) and thermodynamically (-7.0 kcal mol⁻¹) the least favorable of the three possible [3+2] reactions. The [2+2] ethylene addition route to the Os=O and Os=CH₂ double bonds proceeds via initial rearrangement of **1** to the osmaoxirane **1a**. The **1**→**1a** rearrangement as well as the following [2+2] additions have significantly higher activation barriers (>30 kcal mol⁻¹) than the [3+2] reactions. Another isomer of **1** is the dioxosma-cyclopropane **1b** which is 56.2 kcal mol⁻¹ lower in energy and accessible after passing a barrier of 15.7 kcal mol⁻¹ connected with **TS1**→**1b**. The calculations predict that there are no energetically favorable addition reactions of ethylene to **1b**. The isomeric form **1c**, which has a peroxy group, is too high in energy to be relevant for the reaction course. The reliability of the B3LYP/II level of DFT to describe the energy regime for the present system is supported by high level benchmark calculations for a selected set of species performed at the CCSD(T)/II level of post-HF theory.

Acknowledgement

This work was supported by the Deutsche Forschungsgemeinschaft. The generous allotment of computer time by the computation and communication centre of the RWTH Aachen, the CSC Frankfurt, the HHLR Darmstadt, the HLR Stuttgart, as well as excellent service by the HRZ Marburg is gratefully acknowledged.

- [1] M. Schröder, *Chem. Rev.* **1980**, *80*, 187.
- [2] a) S. G. Hentges, K. B. Sharpless, *J. Am. Chem. Soc.* **1980**, *102*, 4263; b) review: H. C. Kolb, M. S. Van Nieuwenhze, K. B. Sharpless, *Chem. Rev.* **1994**, *94*, 2483.
- [3] a) U. Pidun, C. Boehme, G. Frenking, *Angew. Chem.* **1996**, *108*, 3008; *Angew. Chem. Int. Ed. Engl.* **1996**, *35*, 2817; b) S. Dapprich, G. Ujaque, F. Maseras, A. Lledós, D. G. Musaev, K. Morokuma, *J. Am. Chem. Soc.* **1996**, *118*, 11660; c) A. M. Torrent, L. Deng, M. Duran, M. Sola, T. Ziegler, *Organometallics* **1997**, *16*, 13; d) A. J. Del Monte, J. Haller, K. N. Houk, K. B. Sharpless, D. A. Singleton, T. Strassner, A. A. Thomas, *J. Am. Chem. Soc.* **1997**, *119*, 9907; e) J. Frunzke, C. Loschen, G. Frenking, *J. Am. Chem. Soc.* **2004**, *126*, 3642.
- [4] a) G. Li, H.-T. Chang, K. B. Sharpless, *Angew. Chem.* **1996**, *108*, 449; *Angew. Chem. Int. Ed. Engl.* **1996**, *35*, 451. Reviews: b) J. A. Bodkin, M. D. McLeod, *J. Chem. Soc. Perkin Trans. 1* **2002**, 2733; c) K. Muñiz, *Chem. Soc. Rev.* **2004**, *33*, 166.
- [5] D. V. Deubel, K. Muñiz, *Chem. Eur. J.* **2004**, *10*, 2475.
- [6] a) K. Muñiz, M. Nieger, H. Mansikkamäki, *Angew. Chem.* **2003**, *115*, 6140; *Angew. Chem. Int. Ed.* **2003**, *42*, 5958; b) K. Muñiz, A. Iesato, M. Nieger, *Chem. Eur. J.* **2003**, *9*, 5581.
- [7] D. V. Deubel, G. Frenking, *Acc. Chem. Res.* **2003**, *36*, 645.
- [8] a) X. Chen, X. Zhang, P. Chen, *Angew. Chem.* **2003**, *115*, 3928; *Angew. Chem. Int. Ed.* **2003**, *42*, 3798; b) X. Chen, X. Zhang, P. Chen, *Organometallics* **2004**, *23*, 3437; c) S. Narancic, P. Chen, *Organometallics* **2005**, *24*, 10.
- [9] a) A. D. Becke, *J. Chem. Phys.* **1993**, *98*, 5648; b) A. D. Becke, *Phys. Rev. A* **1988**, *38*, 3098; c) C. Lee, W. Yang, R. G. Parr, *Phys. Rev. B* **1988**, *37*, 785.
- [10] P. J. Stevens, F. J. Devlin, Chabalowski, M. J. Frisch, *J. Phys. Chem.* **1994**, *98*, 11623.
- [11] Gaussian 03, Revision C.02, M. J. Frisch, G. W. Trucks, H. B. Schlegel, G. E. Scuseria, M. A. Robb, J. R. Cheeseman, J. A. Montgomery, Jr., T. Vreven, K. N. Kudin, J. C. Burant, J. M. Millam, S. S. Iyengar, J. Tomasi, V. Barone, B. Mennucci, M. Cossi, G. Scalmani, N. Rega, G. A. Petersson, H. Nakatsuji, M. Hada, M. Ehara, K. Toyota, R. Fukuda, J. Hasegawa, M. Ishida, T. Nakajima, Y. Honda, O. Kitao, H. Nakai, M. Klene, X. Li, J. E. Knox, H. P. Hratchian, J. B. Cross, V. Bakken, C. Adamo, J. Jaramillo, R. Gomperts, R. E. Stratmann, O. Yazyev, A. J. Austin, R. Cammi, C. Pomelli, J. W. Ochterski, P. Y. Ayala, K. Morokuma, G. A. Voth, P. Salvador, J. J. Dannenberg, V. G. Zakrzewski, S. Dapprich, A. D. Daniels, M. C. Strain, O. Farkas, D. K. Malick, A. D. Rabuck, K. Raghavachari, J. B. Foresman, J. V. Ortiz, Q. Cui, A. G. Baboul, S. Clifford, J. Cioslowski, B. B. Stefanov, G. Liu, A. Liashenko, P. Piskorz, I. Komaromi, R. L. Martin, D. J. Fox, T. Keith, M. A. Al-Laham, C. Y. Peng,

- A. Nanayakkara, M. Challacombe, P. M. W. Gill, B. Johnson, W. Chen, M. W. Wong, C. Gonzalez, J. A. Pople, Gaussian, Inc., Wallingford CT, **2004**.
- [12] A. Schäfer, C. Huber, R. Ahlrichs, *J. Chem. Phys.* **1994**, *100*, 5829.
- [13] D. Andrae, U. Haeussermann, M. Dolg, H. Stoll, H. Preuss, *Theor. Chim. Acta* **1990**, *77*, 123.
- [14] J. M. L. Martin, A. Sundermann, *J. Chem. Phys.* **2001**, *114*, 3408.
- [15] T. H. Dunning, *J. Chem. Phys.* **1989**, *90*, 1007.
- [16] a) H. Raghavachari, G. W. Trucks, J. A. Pople, M. Head-Gordon, *Chem. Phys. Lett.* **1989**, *157*, 479; b) J. D. Watts, J. Gauss, R. J. Bartlett, *J. Chem. Phys.* **1993**, *98*, 8718; c) C. Hampel, K. Peterson, H.-J. Werner, *Chem. Phys. Lett.* **1992**, *190*, 1; d) M. J. O. Deegan, P. J. Knowles, *Chem. Phys. Lett.* **1994**, *227*, 321.
- [17] MOLPRO, a package of ab initio programs designed by H.-J. Werner, P. J. Knowles, version 2002.6, R. D. Amos, A. Bernhardsson, A. Berning, P. Celani, D. L. Cooper, M. J. O. Deegan, A. J. Dobbyn, F. Eckert, C. Hampel, G. Hetzer, P. J. Knowles, T. Korona, R. Lindh, A. W. Lloyd, S. J. McNicholas, F. R. Manby, W. Meyer, M. E. Mura, A. Nicklass, P. Palmieri, R. Pitzer, G. Rauhut, M. Schütz, U. Schumann, H. Stoll, A. J. Stone, R. Tarroni, T. Thorsteinsson, H.-J. Werner.
- [18] D. V. Deubel, S. Schlecht, G. Frenking, *J. Am. Chem. Soc.* **2001**, *123*, 10085.
- [19] G. Erker, U. Dorf, P. Czisch, J. L. Petersen, *Organometallics* **1986**, *5*, 668, and references therein.
- [20] a) A. Fürstner, D. N. Jumbam, *Tetrahedron* **1992**, *48*, 5991; b) A. Fürstner, A. Hupperts, A. Ptock, E. Janssen, *J. Org. Chem.* **1994**, *59*, 5215; c) B. Bogdanovic, A. Bolte, *J. Organomet. Chem.* **1995**, *502*, 109.
- [21] M. Stahl, U. Pidun, G. Frenking, *Angew. Chem.* **1997**, *109*, 2308; *Angew. Chem. Int. Ed. Engl.* **1997**, *36*, 2234.
- [22] T. J. Lee, P. R. Taylor, *Int. J. Quantum Chem. Symp.* **1989**, *23*, 199.
- [23] P. R. Taylor in *Lecture Notes in Quantum Chemistry II* (Ed.: B. O. Roos), Springer, Berlin, **1994**, p. 125 ff.

Received: February 25, 2005
Published online: May 25, 2005